



Cite this: *New J. Chem.*, 2020, **44**, 210

Anisotropic and magnetic properties in non-metal and non-radical organic aggregates of tri-substituted phenyl derivatives†

Nur Amanina Juniasari Tun Nur Iskandar,^a Yeap Guan-Yeow,^{id}*^a Nobuyuki Maeta,^b Masato M. Ito,^{id}^b Yoshiyuki Nakamura,^c Katarzyna Gas,^{id}^d and Maciej Sawicki^{id}^d

A new series of tri-substituted phenyl derivatives containing an aromatic imine unit and biphenyl ester possessing various numbers of carbon atoms at the terminal alkoxy chain, OC_nH_{2n+1} ($n = 7-12$), along with a lateral *o*-ethoxy substituent have been successfully prepared and characterised by CHN microanalysis along with spectroscopic techniques (FTIR, 1H - and ^{13}C -NMR). The texture observation under polarized light revealed that all the soft condensed materials exhibited an enantiotropic nematic (N) phase. The current studies have shown that the mesomorphic behaviour is greatly influenced by the length of the alkoxy chains wherein the thermal stability of a tri-substituted phenyl derivative will decrease if the terminal alkoxy chain is increased from $n = 7$ to 12. For the first time, these materials which do not possess any magnetic species in their structure, demonstrate magnetic interaction through naked eye observation as well as quantitative measurement using a SQUID magnetometer.

Received 26th May 2019,
Accepted 20th November 2019

DOI: 10.1039/c9nj02730k

rsc.li/njc

1. Introduction

A wide range of materials in the state of matter that cannot be classified merely as crystalline solids or simple liquids are generally known as soft condensed materials.¹ There are various forms of soft condensed materials including the fourth unique state of matter which is liquid crystals.² It has been well established that the vital requirement for a compound to exhibit liquid crystalline behaviour depends on the structure of the compound. The materials usually consist of rod-like rigid units, terminal and lateral substituents that are packed in a parallel manner^{3,4} and large molecular length-to-breadth ratio.⁵ One of these works had focussed on the influence of different terminal alkoxy chains on the Schiff base esters in which the lengthening of the terminal alkoxy chains lengths resulted in a significant effect on the mesomorphic behaviour.⁶ Recently, a study on the effect of various alkyloxy chains on the heterocyclic derivative having an ester-chalcone central linkage has shown that the

shortest terminal chain ($n = 10$) displayed the absence of mesomorphic property, while the remaining homologues ($n = 12-16$) exhibit an enantiotropic SmA phase. They also revealed that both the phase transition temperatures and the mesophase temperature range were also influenced by the length of the terminal chains.⁷ Besides, the appearance of enantiotropic mesophases, namely N and Sm phases has been observed in the higher membered chains.⁸

Since more than a decade ago, the physical properties and mesomorphic behaviour of these compounds have been associated with the influence brought about by the presence of the substituent at the strategic position in the central core.^{9,10} In general, the lateral substituent reduces both the clearing and melting temperature by broadening the core of the mesogen.¹¹ For instance, the fluoro lateral substituents are frequently employed in liquid crystal (LC) systems to suppress the presence of the smectogenic phase in forming an N phase that exhibits low melting temperature.¹² A review on the influence of two homologous series with chloro and methyl lateral groups showed that the chloro lateral group displayed N and Sm phases while the methyl group only exhibited an N phase.¹³ Comparison studies of both lateral substituents with structurally related homologous series revealed that the increase in the breadth of mesogens with the lateral group in the *ortho* position led to a decline in the mesophase thermal stability as compared to the unsubstituted analogue. They also stated that the position of both lateral substituents influenced the thermal stability and mesomorphic behaviour.^{13,14} It has been reported that the melting

^a Liquid Crystal Research Laboratory, School of Chemical Sciences, Universiti Sains Malaysia, 11800 Minden, Penang, Malaysia. E-mail: gyeap@usm.my;
Fax: +(60)-4-6574854

^b Faculty of Science & Engineering, Soka University, 1-236 Tangi-cho, Hachioji, Tokyo 192-8577, Japan

^c Nanospace Catalysis Unit, Institute of Innovative Research, Tokyo Institute of Technology, 4259-S1 Nagatsuta-cho, Midori-ku, Yokohama-shi, Kanagawa, 226-8503, Japan

^d Institute of Physics, Polish Academy of Sciences, Aleja Lotnikow 32/46 PL-02668, Warsaw, Poland

† Electronic supplementary information (ESI) available. See DOI: 10.1039/c9nj02730k

point of LC monomers comprising a reactive group in the lateral position decreased as the length of the lateral substituent increased with the molecular long axis.¹⁵ Herein, we are prompted to study a new series of tri-substituted phenyls in which a biphenyl ester with various numbers of carbon atoms at the terminal alkoxy chains and an aromatic imine fragment are connected to a central phenyl core along the long axis while an ethoxy group is attached to this phenyl centre at the *ortho* position. Besides, we also attempt to explore the presence of magnetism in these materials which are categorized as non-metal or non-radical substances.

2. Experimental

2.1 Chemicals and reagents

4-(4-Hydroxyphenyl)benzoic acid, 3-ethoxy-4-hydroxybenzaldehyde and *N,N'*-dicyclohexylcarbodiimide (DCC) were purchased from TCI (Tokyo Chemical Industry), Japan. 1-Bromoheptane, 1-bromooctane, 1-bromononane, 1-bromodecane, 1-bromoundecane and 1-bromododecane were obtained from Merck, UK. Potassium hydroxide, glacial acetic acid, 4-(dimethylamino)pyridine (DMAP), ethanol, dichloromethane, *p*-anisidine and diethyl ether were purchased from Sigma Aldrich, USA.

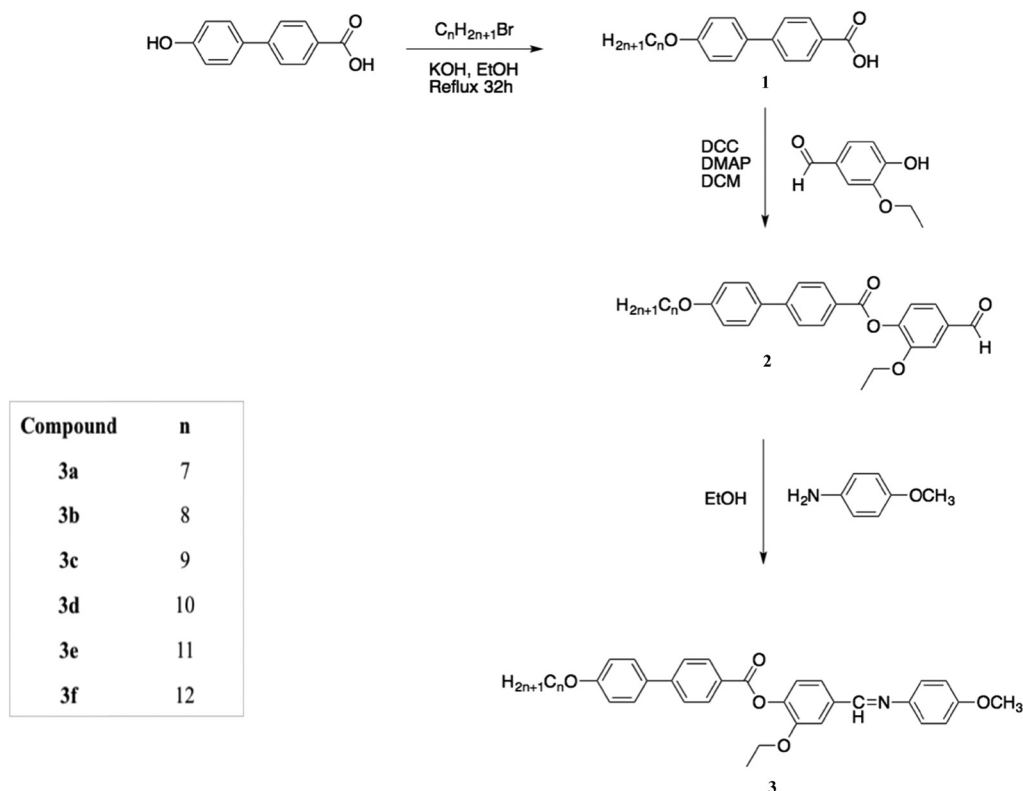
2.2 Physical measurement

The carbon, hydrogen and nitrogen (CHN) microanalyses for all the target compounds were carried out using a PerkinElmer 2400 LS Series CHNS/O analyzer. The FT-IR spectra were recorded using a PerkinElmer 2000 FT-IR spectrophotometer in

the frequency range 400–4000 cm^{-1} . The ^1H and ^{13}C -NMR spectra for the intermediates and target compounds were obtained from the Bruker-Avance 500 MHz spectrometer equipped with ultra-shield magnets. Deuterated chloroform (CDCl_3) and dimethyl sulfoxide (DMSO) were used as the solvents and TMS as the internal standard. Thin-layer chromatography (TLC) was performed with a TLC plate coated with silica and the spots on it were visualised by short wave UV light irradiation. The transition temperatures and associated enthalpy values were measured using Seiko DSC120 model 5500 differential scanning calorimeters available in the Faculty of Engineering, Soka University, Japan with a heating and cooling rate of ± 2 $^\circ\text{C}$. The liquid crystal textures of the target compounds were observed under a Carl Zeiss Axioskop 40 polarising microscope equipped with a Linkam LTS350 hot stage and TMS94 temperature controller at the Liquid Crystal Research Laboratory, School of Chemical Sciences, USM. The attraction of all the title compounds at room temperature was investigated first by direct observation under a permanent magnet. The magnetic phenomenon of a selected compound from this series at variable temperature was further investigated using the superconducting quantum interference device (SQUID) magnetometer MPMS XL5 of Quantum Design at the Institute of Physics, Polish Academy of Sciences, Warsaw, Poland.

2.3 Synthesis

The synthesis of 2-ethoxy-4-(((4-methoxyphenyl)imino)methyl)phenyl-4'-(alkyloxy)-1,1'-biphenyl-4-carboxylate, **3a–3f**, was carried out following Scheme 1. 4'-Alkoxy-4-biphenylcarboxylic acid, **1a–1f**,



Scheme 1 Synthetic route towards the preparation of target compounds **3a–3f**.

was prepared by the etherification reaction between 4'-hydroxy-4-biphenylcarboxylic acid and 1-bromoalkane in the presence of potassium hydroxide in ethanol. The compound thus obtained was reacted subsequently with 3-ethoxy-4-hydroxybenzaldehyde under Steglich esterification conditions using 4-dimethylamino-pyridine (DMAP) and *N,N'*-dicyclohexylcarbodiimide (DCC) to form benzaldehyde derivatives, **2a–2f**. A condensation reaction between the appropriate *p*-anisidine and compounds **2a–2f** in ethanol led to the formation of title compounds **3a–3f**. Detailed discussion on the target compounds **3a–3f** can be based on a representative compound **3c** as these compounds possess identical characteristics.

2.3.1 Synthesis of 4'-alkoxy-4-biphenylcarboxylic acid, 1a–1f. 4'-Hydroxy-4-biphenylcarboxylic acid and potassium hydroxide (KOH) were dissolved in ethanol/water (9/1) in a round bottom flask and the solution was stirred for 20 min. 1-Bromononane was then added dropwise and the mixture was refluxed overnight. Upon completion of the reaction, one equimolar of KOH was added and the mixture was refluxed for another 4 hours. The resulting mixture was left to evaporate at room temperature and the mixture was poured into distilled water and acidified with glacial acetic acid (pH = 2–3). The precipitate thus obtained was filtered off and washed twice with distilled water and diethyl ether. The crude product was recrystallized from glacial acetic acid.

1c: yield 93%. Elemental analysis (%): found, C 78.10, H 8.35; calculated (C₂₂H₂₈O₃), C 77.61, H 8.29. IR (KBr) ν/cm^{-1} , 2929–2857 (C–H alkyl), 1684 (C=O ester), 3006 (O–H). ¹H-NMR (DMSO) δ/ppm , 0.84–0.87 (t, 3H, CH₃), 1.26–1.75 (m, 14H, CH₂), 4.00–4.02 (t, 2H, OCH₂), 7.02 (d, 2H, Ar), 7.66 (d, 2H, Ar), 7.73 (d, 2H, Ar), 7.97 (d, 2H, Ar).

2.3.2 Synthesis of 2-ethoxy-4-formylphenyl-4'-(alkyloxy)-[1,1'-biphenyl]-4-carboxylate, 2a–2f. A mixture of 3-ethoxy-4-hydroxybenzaldehyde, intermediary compound **1c** and 0.32 equivalent of DMAP was dissolved in an appropriate amount of DCM. To this mixture, *N,N'*-dicyclohexylcarbodiimide (DCC) in a minimum amount of DCM was added dropwise and the mixture was stirred overnight at room temperature. The white solid of *N,N'*-dicyclohexylurea was removed by filtration and the filtrate obtained was evaporated at room temperature to remove the remaining solvent. The desired product was recrystallized twice from ethanol to yield a white precipitate.

2c: yield 67%. Elemental analysis (%): found, C 76.75, H 7.51; calculated (C₃₁H₃₆O₅), C 76.20, H 7.43. FTIR ν/cm^{-1} , 2924–2856 (C–H alkyl), 1730 (C=O aldehyde). ¹H NMR (CDCl₃) δ/ppm , 0.87–0.89 (t, 3H, CH₃), 1.46–1.48 (t, 3H, CH₃), 1.28–1.84 (m, 14H, CH₂), 4.00–4.03 (t, 2H, OCH₂), 4.14–4.17 (m, 2H, OCH₂), 6.99 (d, 2H, Ar), 7.35 (d, 1H, Ar), 7.52 (d, 2H, Ar), 7.60 (d, 2H, Ar), 7.69 (d, 2H, Ar), 8.22 (d, 2H, Ar), 9.97 (s, 1H, CHO).

2.3.3 Synthesis of 2-ethoxy-4-(((4-methoxyphenyl)imino)-methyl)phenyl-4'-(alkyloxy)-[1,1'-biphenyl]-4-carboxylate, 3a–3f. An ethanolic solution of 4-methoxyaniline was added dropwise to a stirring hot ethanolic solution of compound **2c** in a round bottom flask. The mixture was refluxed overnight at 70 °C. The white precipitate thus formed was filtered off and recrystallized twice from ethanol.

3c: yield 73%. Elemental analysis (%): found, C 76.96, H 7.33, N 2.51; calculated (C₃₈H₄₃NO₅), C 76.87, H 7.30, N 2.36. FTIR ν/cm^{-1} , 2926–2856 (C–H alkyl), 1605 (C=N), 1729 (C=O ester). ¹H NMR (DMSO) δ/ppm , 0.85–0.88 (t, 3H, CH₃), 1.40–1.45 (m, 3H, CH₃), 1.23–1.77 (m, 14H, CH₂), 3.79 (s, 3H, OCH₃), 4.02–4.05 (t, 2H, OCH₂), 4.13–4.17 (q, 2H, OCH₂), 7.00 (d, 2H, Ar), 7.07 (d, 2H, Ar), 7.32 (d, 2H, Ar), 7.39 (d, 1H, Ar), 7.55 (d, 1H, Ar), 7.72 (t, 3H, Ar), 7.87 (d, 2H, Ar), 8.17 (d, 2H, Ar), 8.66 (s, 1H, CH=N).

2.4 Magnetic measurements

Magnetic studies are performed using the commercial superconducting quantum interference device (SQUID) magnetometer MPMS XL5 of Quantum Design. To facilitate SQUID measurements of powdered samples of expected weak signal, without introducing strong signals of gelatine capsules or other unreliable carriers, the powdered samples were stabilized by mixing them with a strongly diluted GE-varnish. Subsequently, these mixtures were transferred into 5 × 4 × 0.15 mm³ pieces of previously well magnetically characterized silicon (Si), to provide a solid support and to ease the sample handling at the same time. Then, such an open sandwich was attached to the center of a long silicon strip and the whole arrangement was lowered into the SQUID sample chamber. The preparation procedure for representative compound **3f** is exemplified in the ESI.† All the measurements, data reduction and final magnetic moment determination were performed by strictly following the already described procedures adequate for high sensitivity studies of samples of minute magnetic signals.¹⁶

3. Results and discussion

3.1 Chemical composition

The chemical composition of title compounds **3a–3f** can be inferred from the CHN microanalytical data (Table 1). It is apparent that all the compounds **3a–3f** exhibit high purity because the composition of C, H and N as derived from experimental data is in good agreement with the calculated values.

3.2 FT-IR spectroscopy studies

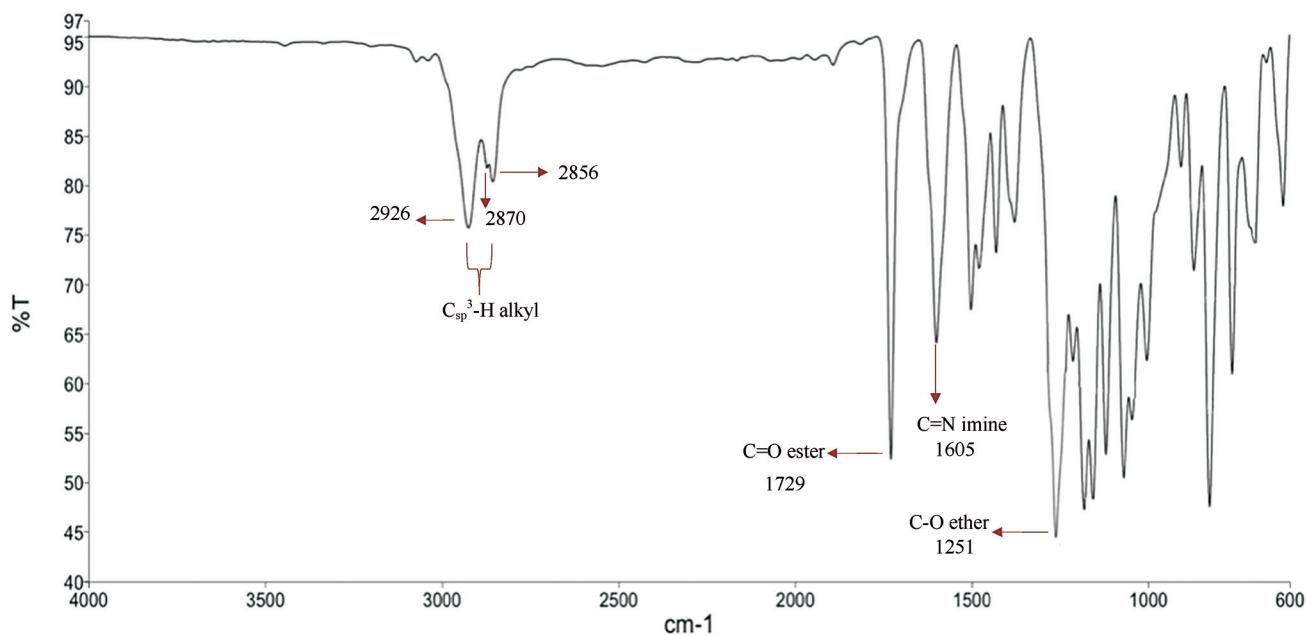
The FT-IR data for **3a–3f** show that the stretching frequency for C_{sp³}-H of elongated terminal groups attached to the biphenyl rings appeared at 2926–2856 cm⁻¹.¹⁷ A weak absorption band at 2870 cm⁻¹ is due to the presence of an ethoxy group at the phenyl ring. The C–O stretching for the ether group displayed a signal at 1251 cm⁻¹ while the stretching vibration of C=O for the ester group showed a strong absorption band at 1729 cm⁻¹. An absorption band with a strong intensity at 1605 cm⁻¹ can be ascribed to C=N of the imine group. The FT-IR spectrum of representative compound **3c** is illustrated in Fig. 1 for clarity.

3.3 ¹H and ¹³C-NMR spectroscopy studies

Since the NMR spectra for **3a–3f** show identical splitting patterns, the assignment of these compounds can be described using the spectra of representative compound **3c**. ¹H and ¹³C-NMR

Table 1 Molecular formulas, molecular weight (MW), percentage yields (%) and CHN microanalytical values for title compounds **3a–3f**

Compounds	Molecular formulas	MW	% Yield	% C ^a	% H ^a	% N ^a
3a	C ₃₆ H ₃₉ NO ₅	565.71	65	76.85 (76.43)	6.99 (6.95)	2.68 (2.48)
3b	C ₃₇ H ₄₁ NO ₅	579.74	58	76.84 (76.66)	7.15 (7.13)	2.54 (2.42)
3c	C ₃₈ H ₄₃ NO ₅	593.76	73	76.96 (76.87)	7.33 (7.30)	2.51 (2.36)
3d	C ₃₉ H ₄₅ NO ₅	607.79	81	77.09 (77.07)	7.48 (7.46)	2.40 (2.30)
3e	C ₄₀ H ₄₇ NO ₅	621.82	58	77.67 (77.26)	7.66 (7.62)	2.47 (2.25)
3f	C ₄₁ H ₄₉ NO ₅	635.85	56	77.55 (77.45)	7.80 (7.77)	2.29 (2.20)

**Fig. 1** FT-IR spectrum of representative compound **3c**.

spectra of compound **3c** and its molecular structure with complete atomic numbering are shown in Fig. 2 and 3.

The methylene proton from the nonyloxy chains (H2–H8) gave rise to several sets of multiplets at $\delta = 1.23$ – 1.34 ppm and $\delta = 1.71$ – 1.77 ppm. The signals assignable to the methyl proton at the terminal ethoxy chains (H38) overlapped leading to a multiplet at $\delta = 1.40$ – 1.45 ppm. The appearance of an intense singlet at $\delta = 3.79$ ppm was attributed to the proton H36 from the methoxy group. A triplet at $\delta = 4.02$ – 4.05 ppm can be ascribed to the oxymethylene protons at the terminal nonyloxy chains (H9) whilst a quartet observed at $\delta = 4.13$ – 4.17 ppm was assigned to the oxymethylene protons of ethoxy chains at the *ortho* position (H37). The aromatic protons H19&H20 appeared as a doublet at $\delta = 8.17$ ppm. These protons appeared at a more downfield region than the other biphenyl aromatic protons owing to the diamagnetic anisotropic effect of the ester group. Six doublet signals resonated at $\delta = 7.00$, 7.07 , 7.32 , 7.39 , 7.55 and 7.87 ppm can be ascribed to H33&H34, H11&H12, H31&H32, H24, H26 and H17&H18, respectively. The signal attributed to H13&H14 seemed to appear as a triplet instead of a doublet and this could probably be due to the overlapping with the signal of H27.

The proton from the imine group (H29) appeared at $\delta = 8.66$ ppm as a singlet. This proton was observed at the most downfield

region due to the effect of the π bond of sp^2 hybridization and the electron-withdrawing group of the nitrogen atom.

From Fig. 3, the peak at $\delta = 159.95$ ppm can be ascribed to the carbon C29 which was attached to the nitrogen atom in the C=N group whereas several peaks observed at $\delta = 115.63$, 129.10 , 127.97 , 130.14 , 123.89 , 122.26 , 112.98 , 123.00 and 115.08 ppm were attributed to the aromatic carbons of C11&C12, C13&C14, C17&C18, C19&C20, C24, C26, C27, C31&C32 and C33&C34, respectively. The signals that emerged at $\delta = 14.20$, 56.03 and 14.96 ppm suggest that these peaks can be ascribed to the carbons C1, C36 and C38, respectively. Meanwhile, the methylene carbons C2–C8 were found to appear in the upfield region of $\delta = 21.97$ – 32.17 ppm. The resonances due to carbon from the oxymethylene group, C9 and C37, were observed at $\delta = 64.16$ and 67.87 ppm, respectively.

3.4 Mesomorphic behaviour

The mesophase behaviour of all target compounds **3a–3f** was observed under a polarizing optical microscope (POM) on heating and cooling cycles. The POM observation revealed that all the title compounds **3a–3f** display an enantiotropic nematic (N) phase. The nematic phase associated with these compounds has been substantiated by the texture observation wherein the development of N droplets coalesced into the schlieren texture

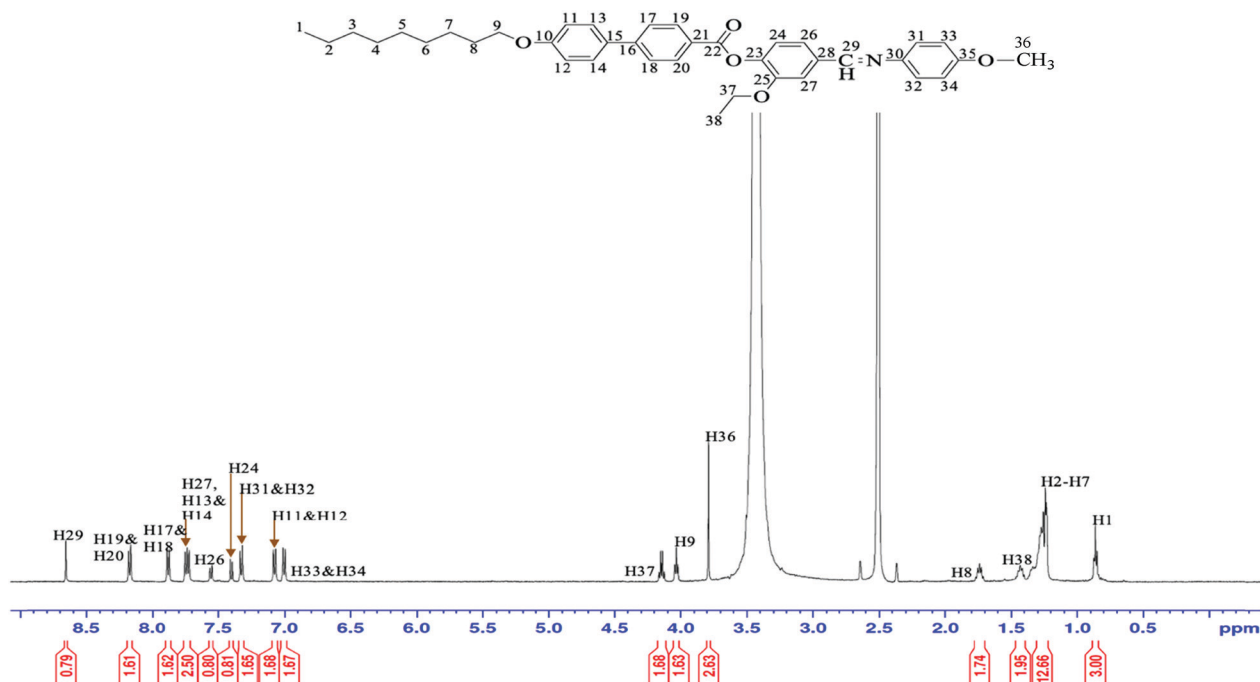


Fig. 2 ^1H -NMR spectrum of representative compound **3c**.

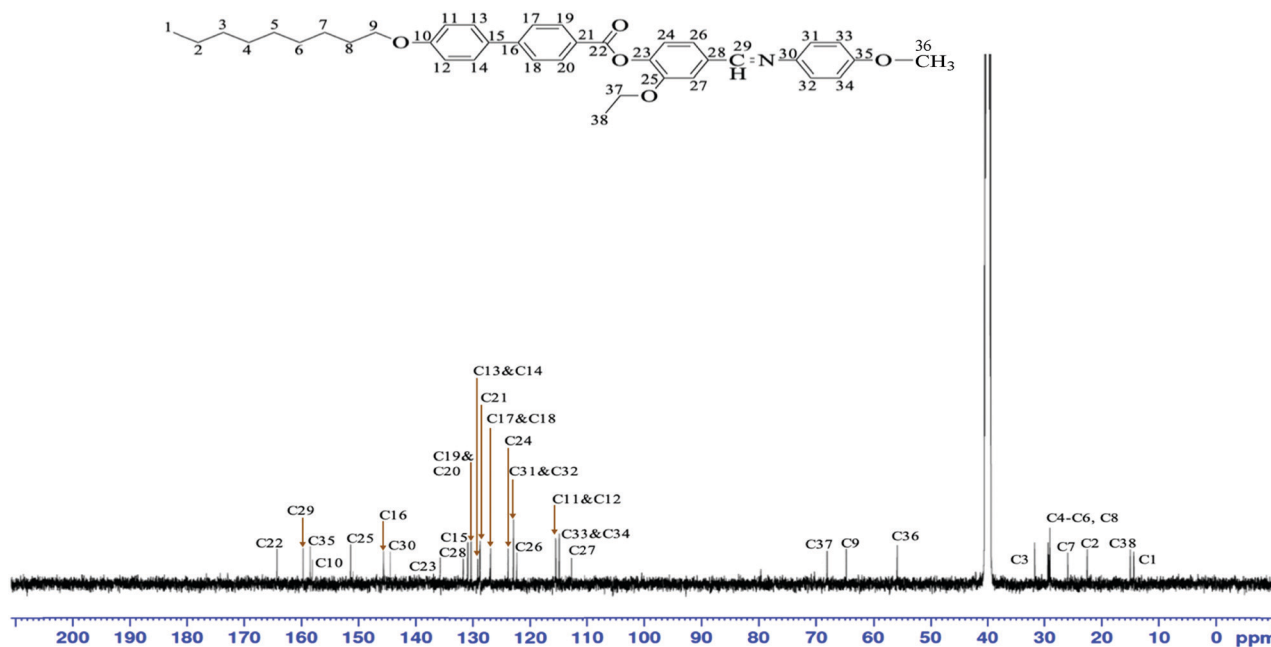


Fig. 3 ^{13}C -NMR spectrum of representative compound **3c**.

with two-brush and four-brush defects is presented for representative compound **3d** in Fig. 4. Upon heating, the compound **3d** shows a crystal to crystal (Cr_1 - Cr_2) phase transition at 118.4 °C. The continuous heating has led to the transformation of the Cr_2 phase into a schlieren texture of the N phase at 240.0 °C. Subsequently, isotropization occurred at 244.8 °C. The formation of N droplets which coalesced into the schlieren texture with two-brush and four-brush defects is observed at

238.4 °C upon cooling. On further cooling, only crystallization is observed.

The phase sequence for all target compounds **3a**-**3f** was further confirmed by the DSC experiment. The transition temperatures and associated enthalpy values of these compounds are tabulated in Table 2. Fig. 5 illustrates a DSC thermogram of representative compound **3e**. Upon heating, two endothermic peaks representing Cr-N and N-I transitions were observed at

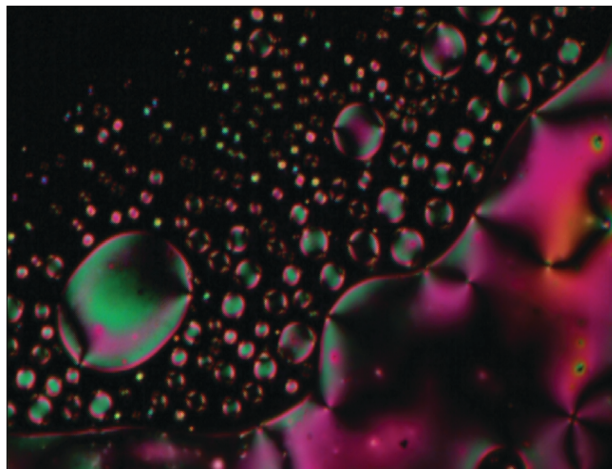


Fig. 4 Photomicrograph showing nematic droplets coalesce into the schlieren texture with two-brush and four-brush defects of compound **3d** at 238.4 °C upon cooling.

Table 2 Phase transition temperatures (°C) and associated enthalpy values (kJ mol⁻¹, in parentheses) of compounds **3a–3f**

Compound	<i>n</i>	Cr ₁	Cr ₂	N	I
3a	7	• 125.3 ^a	• 249.3 (54.3)	• 266.1 (1.9)	•
		• 124.1 ^a	• 248.6 (–24.1)	• 264.3 (–1.6)	•
3b	8	• 124.4 ^a	• 244.9 (51.2)	• 260.9 (1.8)	•
		• 123.9 ^a	• 241.8 (–22.1)	• 258.0 (–1.3)	•
3c	9	• 124.1 ^a	• 240.7 (47.9)	• 253.9 (2.2)	•
		• 121.7 ^a	• 238.1 (–23.2)	• 250.8 (–1.7)	•
3d	10	• 118.4 ^a	• 233.5 (45.6)	• 242.0 (2.1)	•
		• 111.9 ^a	• 230.3 (–23.7)	• 237.6 (–1.5)	•
3e	11	• 123.3 ^a	• 232.9 (50.6)	• 239.8 (2.0)	•
		• 116.8 ^a	• 229.8 (–37.8)	• 237.6 (–1.4)	•
3f	12	• 121.4 ^a	• 231.0 (41.7)	• 234.1 (2.7)	•
		• 116.8 ^a	• 227.7 (–38.6)	• 233.9 (–1.9)	•

Cr₁ = crystal 1; Cr₂ = crystal 2; N = nematic phase; I = isotropic.

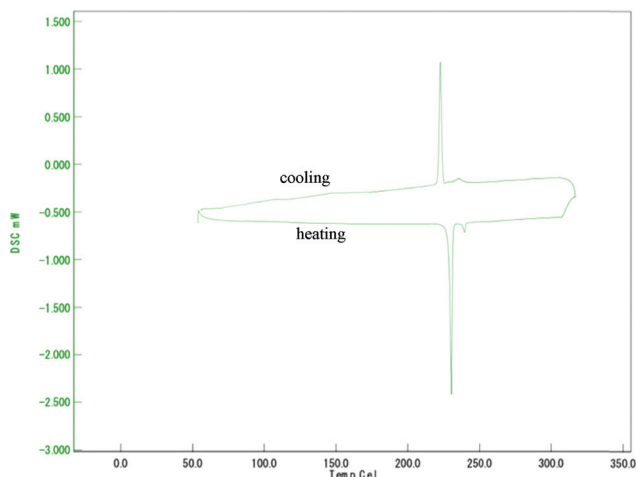


Fig. 5 DSC thermogram of compound **3e** upon heating and cooling cycles.

232.9 °C and 239.8 °C with enthalpy (ΔH) values of 50.6 kJ mol⁻¹ and 2.0 kJ mol⁻¹, respectively. Upon cooling, two exothermic peaks emerged at 237.6 °C and 229.8 °C with respective enthalpy

values of $\Delta H = -1.4$ kJ mol⁻¹ and -37.8 kJ mol⁻¹ assignable to the I–N and N–Cr transitions. The peak ascribed to the transition of Cr₁–Cr₂ upon both heating and cooling is found to be weak and therefore unnoticed under the DSC thermogram. However, the Cr₁–Cr₂ transition is observable under the POM.

Fig. 6 shows a plot of transition temperatures *versus* the number of carbon atoms in the alkoxy chain, *n*, for the title compounds **3a–3f**. As shown in Fig. 6, the melting point (Cr₂–N) apparently decreased from 249.3 °C (**3a**) to 231.0 °C (**3f**) on lengthening the terminal alkoxy chains. This observation is due to compound **3a** which has comparatively high rigidity and relatively low length-to-breadth ratio among these compounds **3b–3f** which favours a rigid rod conformation. This conformation promotes the binding forces between the molecules that are positioned in an orderly manner in the crystal lattice.¹⁸ Likewise, it also can be implied from Fig. 6 that the clearing temperature decreased as the terminal chains increased. This descending trend could be due to the dilution of the interaction between the mesogenic cores resulting from the flexibility owing to the longer terminal chains.^{19,20} Compound **3a** has the highest clearing temperature at 266.1 °C wherein the enthalpy value ΔH is 1.9 kJ mol⁻¹ while compound **3f** has the lowest clearing temperature at 234.1 °C with $\Delta H = 2.7$ kJ mol⁻¹. A noticeable feature among all the target compounds is that compound **3a** is thermally more stable than the other title compounds **3b–3f**. This indicates that the tri-substituted phenyl derivatives with a shorter terminal alkoxy chain were thermally more stable and the trend follows the order of $n = 7 > 8 > 9 > 10 > 11 > 12$.

Besides, the length of the terminal chains influenced the thermal stabilities of the mesomorphic behaviour in which the long terminal alkoxy chains led to a reduction in the N thermal stability.²¹ Significant decreases in the temperature range of N phase from 16.8 °C (**3a**) to 3.1 °C (**3f**) can be observed for all the target compounds by lengthening the terminal alkoxy chains. This phenomenon is due to the lengthy carbon chain being attracted and intertwined, facilitating the lamellar molecular packing of this compounds leading to a low N phase temperature range.^{22–24}

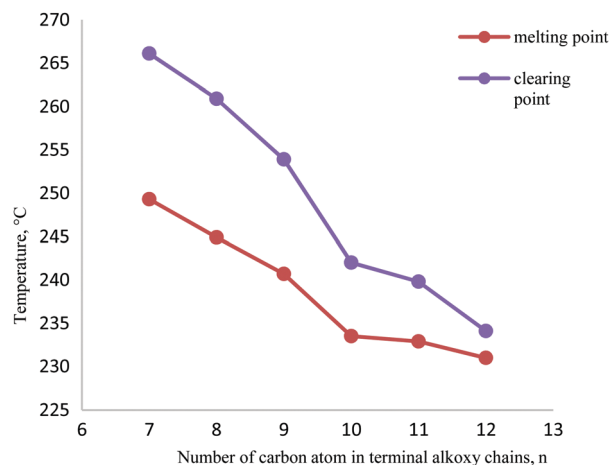


Fig. 6 A plot of transition temperature *versus* the number of carbon atoms in the alkoxy chain for title compounds **3a–3f**.

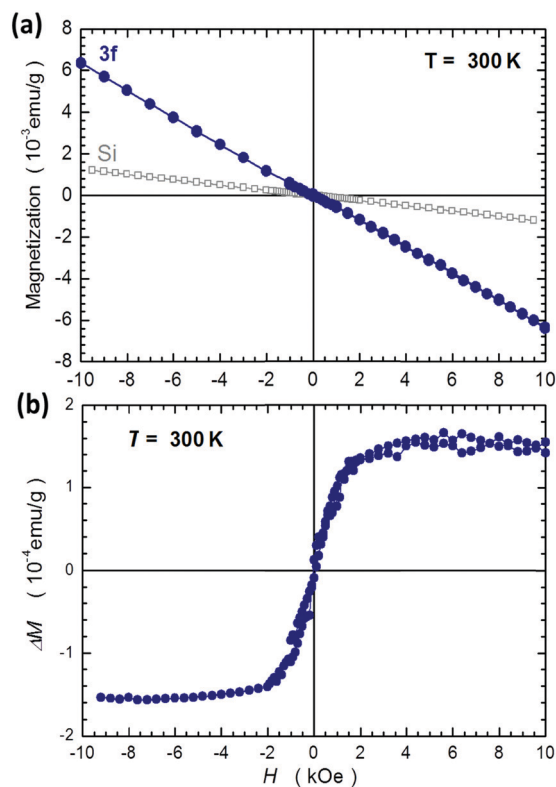


Fig. 7 (a) A comparison of the room temperature magnetic response of the sample **3f** with the response of the Si support on which the sample was deposited. The observed diamagnetic signal in the **3f** sample is approximately 5 times stronger than that of Si. (b) The nonlinear, superparamagnetic-like, part $\Delta M(H)$ present in panel (a) magnetization of sample **3f**.

3.5 Magnetic properties

In addition, the study of these liquid crystalline materials has also been explored to show some unique features of magnetic behaviour. As far as the magnetism is concerned, it has always been associated with the presence of metal or rare-earth elements and organic radical compounds.^{25,26} For the first time, the magnetism arises from these purely organic materials **3a–3f** without having magnetic species capable of exhibiting magnetic behaviour. The magnetic character of the present material can be observed straightforwardly, without resorting to any advanced techniques. As indicated in the ESI,[†] a solid sample of the representative compound **3f**, which is a purely organic substance, is attracted to the weak permanent magnet. The sample remains attached to the magnet unless an external force is applied to detach it. The magnetic response is even better documented by another experiment in which a sample of the same compound is placed on the surface of water, when it flows without any restriction (ESI[†]). This magnetic attraction is observed at room temperature for the solid sample of a few millimeters across and the same magnet is positioned in close proximity to the sample. Comparing the lowest homolog **3a** and highest member **3f**, compound **3f** exhibits stronger magnetic behaviour than compound **3a**. Therefore, the elongation of the length of the terminal alkoxy chains from $n = 7$ to $n = 12$ has contributed to the greater magnetic response.

To quantify the strength of the magnetic response, we measured the room temperature magnetization M of the sample **3f** using SQUID magnetometry in magnetic fields H up to 10 kOe. The main result obtained from these studies is that the sample **3f** is predominantly diamagnetic (M is linear in H with a negative slope) and that its diamagnetic susceptibility, $\chi_{\text{dia}} = -6.3 \times 10^{-7} \text{ emu g}^{-1}$, is approximately 5 times stronger than that of Si, as presented in Fig. 7(a).

The additional magnetic contribution to M can only be revealed by numerical subtraction of the diamagnetic signal, which we approximate as $M_{\text{dia}}(H) = \chi_{\text{dia}}H$. The resulting signal $\Delta M(H) = M(H) - M_{\text{dia}}(H)$ is presented in Fig. 7(b), which clearly exhibits a ferromagnetic-like character. Generally, the behavior presented in Fig. 7(b) can be classified as superparamagnetic-like, which is indicative of the presence of swiftly magnetizing large spins (macrospins) originating from some magnetically coupled volumes of a currently unspecified configuration. It is assumed that a mutual coupling (probably by magnetic dipolar interaction) among these magnetic configurations is responsible for the observed shape of $\Delta M(H)$. It is noted that the reported signal is rather weak, nevertheless, the magnetism is clearly observed in the specimen, despite the fact that magnetic species like transition metals, rare-earth elements or organic radical elements are absent in these target compounds.

4. Conclusions

New tri-substituted phenyl derivatives with different alkoxy chains on the terminal of the biphenyl ester and an aromatic imine system containing an *o*-ethoxy substituent were successfully prepared and characterised. All the title compounds **3a–3f** exhibit the enantiotropic N phase. The flexible terminal alkoxy chains have a strong influence on the thermal stabilities and exhibit a mesomorphic behaviour in which the long terminal alkoxy chains led to a reduction in the thermal stability. Surprisingly, we have uncovered for the first time the magnetic behaviour of non-magnetic species of compounds **3a–3f**. Through observation by the naked eye, an unusual short-range magnetic interaction in which the title compounds **3a–3f** were attracted to the magnet in the solid state was observed. In addition, these compounds were also attracted to the magnet in the presence of a water surface at room temperature. The studies have also shown that longer terminal alkoxy chains seem to give rise to a greater magnetic behaviour. Most importantly, the magnetic response has been observed in these compounds without having any magnetic species deliberately introduced into their structures.

Conflicts of interest

There are no conflicts to declare.

Acknowledgements

The main author (G.-Y. Yeap) would like to thank Universiti Sains Malaysia for providing the research facilities and partial

financial support through Research University RU Grant No. 1001/PKIMIA/8011034.

References

- 1 R. A. Jones, *Soft condensed matter*, Oxford University Press, New York, USA, 2002.
- 2 M. Doi, *Soft matter physics*, Oxford University Press, New York, USA, 2013.
- 3 B. T. Thaker, Y. T. Dhimmarr, B. S. Patel, D. B. Solanki, N. B. Patel, N. J. Chothani and J. B. Kanojiya, Studies Of Calamitic Liquid Crystalline Compounds Involving Ester-Azo Central Linkages With A Biphenyl Moiety, *Mol. Cryst. Liq. Cryst.*, 2011, **548**(1), 172–191.
- 4 M. R. Karim, M. R. K. Sheikh, R. Yahya, N. Mohamad Salleh, K. M. Lo and H. E. Mahmud, The Effect Of Terminal Substituents On Crystal Structure, Mesophase Behaviour And Optical Property Of Azo-Ester Linked Materials, *Liq. Cryst.*, 2016, **43**(12), 1862–1874.
- 5 I. A. Mohammed, G. Sankar, M. Khairuddean and A. B. Mohamad, Synthesis And Liquid Crystalline Properties Of New Diols Containing Azomethine Groups, *Molecules*, 2010, **15**(5), 3260–3269.
- 6 N. R. Jber, M. M. Shukur and A. A. Najaf, Schiff Base Liquid Crystals With Terminal Alkoxy Group Synthesis And Thermotropic Properties, *J. Al-Nahrain Univ. Sci.*, 2014, **17**(2), 64–72.
- 7 Y. W. C. Lim, S. T. Ha, G. Y. Yeap and S. S. Sastry, Synthesis And Mesomorphic Properties Of New Heterocyclic Liquid Crystals With Central Ester–Chalcone Linkages, *J. Taibah Univ. Sci.*, 2017, **11**(1), 133–140.
- 8 V. S. Sharma and R. B. Patel, Study The Effects Of Terminal Side Chain And–Nitro Group On Mesomorphic Behaviour Of Cinnamate–Chalconyl Based Liquid Crystal, *Mol. Cryst. Liq. Cryst.*, 2017, **643**(1), 1–12.
- 9 A. Yoshizawa, H. Kinbara, T. Narumi, A. Yamaguchi and H. Dewa, Synthesis And Physical Properties Of Novel Liquid Crystal Trimers Containing Resorcinol As A Linking Unit, *Liq. Cryst.*, 2005, **32**(9), 1175–1181.
- 10 S. Dixit, Liquid Crystalline Materials With Lateral Polar Chloro Substituent, *J. Mater. Sci.*, 2017, **5**(6), 1–7.
- 11 M. E. Neubert, *Characterization Of Mesophase Types And Transitions. Liquid Crystals, Experimental Study Of Physical Properties And Phase Transitions*, Cambridge University Press, Cambridge, UK, 2001, pp. 29–64.
- 12 I. A. M. Radini, *The Synthesis And Properties Of Liquid Crystals With Bulky Terminal Groups For Bookshelf Geometry Ferroelectric Mixtures*, PhD thesis, University of Hull, 2010.
- 13 J. S. Dave, P. D. Patel and H. Bhatt, Synthesis And Mesomorphic Characteristics Of Fluoroaniline Derivatives With Different Lateral Groups, *Mol. Cryst. Liq. Cryst.*, 2012, **562**(1), 76–84.
- 14 J. S. Dave, C. B. Upasani and P. D. Patel, Effect Of Lateral Substitution On Mesogenic Properties Of Fluoro Aniline Derivatives, *Mol. Cryst. Liq. Cryst.*, 2010, **533**(1), 73–81.
- 15 J. Q. Xie, G. Hou and R. Sun, Synthesis And Properties Of Liquid Crystal Monomers Containing A Reactive Group In The Lateral Substituent, *Liq. Cryst.*, 2016, **43**(5), 598–605.
- 16 M. Sawicki, W. Stefanowicz and A. Ney, Sensitive SQUID Magnetometry For Studying Nanomagnetism, *Semicond. Sci. Technol.*, 2011, **26**, 064006.
- 17 M. R. Karim, M. R. K. Sheikh, R. Yahya, N. M. Salleh and A. D. Azzahari, Synthesis of polymerizable liquid crystalline monomers and their side chain liquid crystalline polymers bearing azo-ester linked benzothiazole mesogen, *Colloid Polym. Sci.*, 2015, **293**(7), 1923–1935.
- 18 G. Y. Yeap, A. Alshargabi, M. M. Ito, W. A. K. Mahmood and D. Takeuchi, Synthesis And Anisotropic Properties Of Azo-Bridged Benzothiazole-Phenyl Esters, *Mol. Cryst. Liq. Cryst.*, 2012, **557**(1), 126–133.
- 19 B. T. Thaker, B. S. Patel, Y. T. Dhimmarr, D. B. Solnki, N. J. Chothani, N. B. Patel, K. B. Patel and U. Makavana, Synthesis, Characterization And Mesomorphic Properties Of New Rod-Like Thiophene Based Liquid Crystals, *Mol. Cryst. Liq. Cryst.*, 2012, **562**(1), 98–113.
- 20 L. K. Ong and S. T. Ha, Influence Of Linking Group Orientation On Mesomorphism Of Two Aromatic Ring Mesogens, *J. Chem.*, 2013, **2013**, 5.
- 21 C. C. Luo, Y. G. Jia, K. M. Song, F. B. Meng and J. S. Hu, The Effect Of Terminal Alkoxy Chain On Mesophase Behaviour, Optical Property And Structure Of Chiral Liquid Crystal Compounds Derived From (–)-Menthol, *Liq. Cryst.*, 2017, **44**(14–15), 2366–2378.
- 22 K. L. Foo, S. T. Ha and S. L. Lee, Synthesis And Characterization Of Thermotropic Liquid Crystals Consisting Heterocyclic Benzothiazole Core System, *Asian J. Chem.*, 2014, **26**(22), 7627–7631.
- 23 S. T. Ha, T. M. Koh, S. T. Ong, Y. F. Win and Y. Sivasothy, Benzothiazole As Structural Components In Liquid Crystals, *Transworld Research Network*, 2011, **37**(661), 2.
- 24 S. T. Ha, T. M. Koh, S. L. Lee, G. Y. Yeap, H. C. Lin and S. T. Ong, Synthesis Of New Schiff Base Ester Liquid Crystal With A Benzothiazole Core, *Liq. Cryst.*, 2010, **37**, 547–554.
- 25 E. Coronado, P. Delhaès, D. Gatteschi and J. S. Miller, *Molecular Magnetism: From Molecular Assemblies To The Devices*, Springer Science & Business Media, 2013, p. 321.
- 26 J. S. Miller, Organic-and molecule-based magnets, *Mater. Today*, 2014, **17**(5), 224–235.